Dual-Mode Polarization Index Modulation for Polarization Division Multiplexing OWC Systems

Yihan Zhao, Zhihong Zeng, *Member, IEEE*, Xinyue Pan, Chen Chen, *Senior Member, IEEE*, and Harald Haas, *Fellow, IEEE*

***Abstract*—In this Letter, we propose and demonstrate a dual-mode polarization index modulation (DM-PIM) scheme for polarization division multiplexing optical wireless communication (PDM-OWC) systems. By performing dual-mode index modulation in the polarization domain, DM-PIM can transmit both index and constellation bits to enhance the spectral efficiency of PDM-OWC systems. As constellation design plays a vital role in DM-PIM, we further propose and optimize two dual-mode constellations based on pulse amplitude modulation (PAM) format. Since PDM-OWC systems are highly vulnerable to polarization misalignment, we also evaluate the impact of polarization misalignment on the performance of PDM-OWC systems employing different transmission schemes. Experimental results show that DM-PIM with optimized dual-mode PAM constellation exhibits superior bit error rate (BER) performance and strong robustness against polarization misalignment in PDM-OWC systems.**

***Index Terms*—Optical wireless communication, polarization division multiplexing, dual-mode polarization index modulation.**

I. Introduction

IN RECENT years, optical wireless communication (OWC) has been widely emerging as a promising enabling technology for the sixth-generation (6G) of mobile networks, owing to its advantages such as abundant spectrum resource, electromagnetic interference-free operation and high physical-layer security [1]. However, commercial optical elements such as light-emitting diodes (LEDs), laser diodes (LDs) and photo diodes (PDs) are generally bandlimited. The usable bandwidth of these optical elements is small, especially for LEDs which usually have a bandwidth of only a few MHz. To increase the capacity of bandlimited OWC systems, various techniques fully exploiting time, frequency and space domain resources have been widely applied such as spectral-efficient modulation, channel equalization, multiple-input multiple-output (MIMO) transmission, and so on [2], [3], and [4].

Besides, polarization provides an extra degree of freedom for optical signal transmission in OWC systems. On the one hand, polarization shift keying (PolSK) has been applied as an efficient modulation technique for turbulence mitigation in OWC systems, which encodes information bits into different polarization stats of the optical signal [5]. Nevertheless, since no constellation symbols can be transmitted, the spectral efficiency of PolSK is limited by the number of distinguishable polarization stats. On the other hand, polarization division multiplexing (PDM) has been utilized as a spectral-efficient transmission scheme to double the capacity of OWC systems by transmitting two data streams over two orthogonal polarization channels within the same frequency band [6]. However, the performance of PDM-OWC systems is highly affected by the inter-channel crosstalk caused by polarization misalignment between optical transmitter and receiver.

Lately, index modulation has been widely applied for performance improvement in OWC systems, which can be performed in frequency, time, and space domains [7], [8], [9]. Moreover, index modulation can be generally divided into single-mode index modulation (SM-IM) [7], dual-mode index modulation (DM-IM) [9], [10], and multi-mode index modulation (MM-IM) [11], [12]. Specifically, SM-IM is power-efficient and suitable for low signal-to-noise ratio (SNR) applications, while DM-IM and MM-IM are spectral-efficient which are suitable to high-SNR applications. Since MM-IM usually has a high complexity, DM-IM reveals to be a promising candidate to balance spectral efficiency and complexity for bandlimited OWC systems. To the best of our knowledge, DM-IM has not yet been exploited in the polarization domain for OWC systems in the literature.

To further increase the transmission capacity and enhance the robustness against polarization misalignment, in this Letter, we propose and demonstrate a dual-mode polarization index modulation (DM-PIM) scheme for PDM-OWC systems. The main contributions of this work are summarized as follows:

- A DM-PIM scheme is proposed, which not only achieves enhanced transmission capacity as PDM [6] but also adapts to optical point-to-point transmission without suffering from spatial channel correlation as dual-mode spatial index modulation [9].

Received 29 May 2026; revised 10 July 2026; accepted 1 August 2026. Date of publication 4 August 2026; date of current version 14 August 2026. This work was supported in part by the National Natural Science Foundation of China under Grant 62271091 and Grant 62501088; and in part by the Open Research Fund of National Mobile Communications Research Laboratory, Southeast University under Grant 2026D08. *(Corresponding author: Zhihong Zeng.)*

Yihan Zhao, Xinyue Pan, and Chen Chen are with the School of Microelectronics and Communication Engineering, Chongqing University, Chongqing 400044, China (e-mail: 202412131054t@stu.cqu.edu.cn; 20240742@stu.cqu.edu.cn; c.chen@cqu.edu.cn).

Zhihong Zeng is with the School of Microelectronics and Communication Engineering, Chongqing University, Chongqing 400044, China, and also with the National Mobile Communications Research Laboratory, Southeast University, Nanjing 210096, China (e-mail: zhihong.zeng@cqu.edu.cn).

Harald Haas is with the Department of Engineering, Electrical Engineering Division, Cambridge University, CB3 0FA Cambridge, U.K. (e-mail: huh21@cam.ac.uk).

Color versions of one or more figures in this letter are available at https://doi.org/10.1109/LPT.2026.3720287.

Digital Object Identifier 10.1109/LPT.2026.3720287

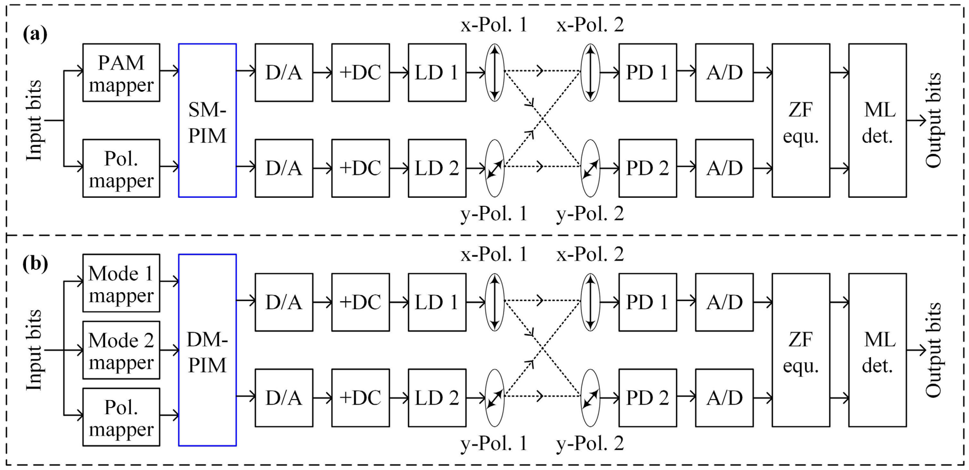

Fig. 1. Schematic diagram of a PDM-OWC system using: (a) SM-PIM, (b) DM-PIM. Pol.: polarization; equ.: equalization; det.: detection.

TABLE I
MAPPING TABLE OF SM-PIM AND DM-PIM

Scheme	Index bit	x-Pol. symbol	y-Pol. symbol
SM-PIM	0	s	0
	1	0	s
DM-PIM	0	s_1	s_2
	1	s_2	s_1

- Two dual-mode constellations based on pulse amplitude modulation (PAM) format are also designed and optimized for DM-PIM based PDM-OWC systems.
- Proof-of-concept experiments are conducted to verify the performance superiority of the proposed DM-PIM scheme over other benchmark schemes in PDM-OWC systems.

II. PRINCIPLE

In this section, we first introduce the principle of the DM-PIM based PDM-OWC system. For the purpose of comparison, single-mode polarization index modulation (SM-PIM) is also introduced as a benchmark scheme for DM-PIM. Figs. 1(a) and (b) depict the schematic diagrams of a PDM-OWC system using SM-PIM and DM-PIM, respectively. For SM-PIM, as shown in Fig. 1(a), the input bits are first divided into two parts including constellation bits and polarization index bits. The constellation bits are fed into the PAM mapper to generate constellation symbols, while the polarization index bits are sent into the polarization mapper to select one from the x-polarization channel and the y-polarization channel to transmit the generated PAM constellation symbols. After that, SM-PIM is performed with respect to the two polarization channels to generate the transmit signal vector. The mapping table of SM-PIM is given in Table I, where one polarization index bit can be additionally transmitted with the PAM constellation symbol s through polarization channel selection. For DM-PIM, as can be seen from Fig. 1(b), there are two mode mappers to generate two distinguishable constellation modes so as to perform DM-IM in the polarization domain. Hence, dual-mode constellation design plays an important role in DM-PIM based PDM-OWC systems, which will be discussed in the following. The mapping table of DM-PIM is also given in Table I, where one polarization index bit can be additionally transmitted with the dual-mode PAM constellation symbols s_1 and s_2 through polarization channel selection.

Letting M_1 and M_2 respectively denote the constellation sizes of mode 1 and mode 2, the spectral efficiency of DM-PIM is $\eta_{\text{DM}} = \log_2 M_1 + \log_2 M_2 + 1$. In contrast, the spectral efficiency of SM-PIM is $\eta_{\text{SM}} = \log_2 M + 1$ where M is the size of the adopted constellation, while the spectral efficiency of PDM is $\eta_{\text{PDM}} = \log_2 M_{\text{x}} + \log_2 M_{\text{y}}$ with M_{x} and M_{y} being the adopted constellation sizes in x-polarization and y-polarization channels respectively.

After performing SM-PIM/DM-PIM, the resultant two digital signals are converted into analog signals via digital-to-analog (D/A) conversion. Subsequently, two direct current (DC) biases are added to generate non-negative signals, which are further used to drive two LDs. The two optical signals pass through a pair of orthogonal polarizers to obtain two orthogonally polarized optical signals for free-space transmission. At the receiving side, a pair of orthogonal polarizers are employed to extract the optical signals in x-polarization and y-polarization channel accordingly for subsequent light detection using PDs. It should be noted that the performance of polarization demultiplexing depends on the polarization alignment between optical transmitter and receiver, and severe inter-channel crosstalk might occur due to polarization misalignment. The PD output analog signals are converted into digital signals via analog-to-digital (A/D) conversion, and the final output bits can be recovered after zero-forcing (ZF) equalization and maximum-likelihood (ML) detection [4]. The computational complexities of ML detection for SM-PIM and DM-PIM are respectively on the orders of $\mathcal{O}(2M)$ and $\mathcal{O}(4M_1M_2)$ per symbol [7], [13].

As discussed above, dual-mode constellation design plays a vital role in the proposed DM-PIM based PDM-OWC system. To this end, we further propose two dual-mode constellation designs based on PAM format. Without loss of generality, we take two 2-PAM sub-constellations as an example to design a composite 4-PAM dual-mode constellation. Fig. 2

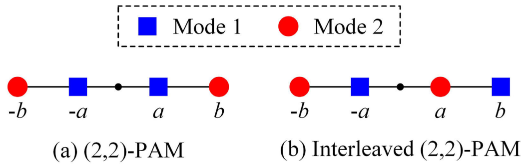

Fig. 2. Constellation design: (a) (2,2)-PAM and (b) interleaved (2,2)-PAM.

illustrates the proposed two dual-mode constellation designs. For the (2,2)-PAM constellation, as shown in Fig. 2(a), mode 1 consists of two inner constellation points with amplitudes of a and $-a$, while mode 2 consists of two outer constellation points with amplitudes of $a+b$ and $-a-b$, with $a>0$ and $b>0$. It can be seen from Fig. 2(a) that the Euclidean distance between two inner constellation points in mode 1 is smaller than that of two outer constellation points in mode 2, leading to imbalanced error performance of two different modes. For the interleaved (2,2)-PAM constellation, as shown in Fig. 2(b), the constellation points of mode 1 and mode 2 are distributed in an interleaved manner where the Euclidean distances between two constellation points in mode 1 and mode 2 become the same, which ensures the comparable error performance of two different modes. Although two low-order PAM constellations are considered, the dual-mode constellation design is generally applicable to higher-order PAM constellations.

With respect to the two dual-mode constellation designs in Fig. 2, the relative positions of constellation points in two modes can be flexibly adjusted so as to optimize the overall error performance of DM-PIM transmission. For the (2,2)-PAM constellation, as shown in Fig. 2(a), the minimum Euclidean distance between two constellation points in the same mode is $2a$ while the Euclidean distance between two adjacent constellation points in two different modes is b. Hence, we can define the amplitude ratio for the (2,2)-PAM constellation as $p_1 = b/2a$. For the interleaved (2,2)-PAM constellation, as illustrated in Fig. 2(b), the Euclidean distance between two constellation points in the same mode is $2a+b$ while the Euclidean distance between two adjacent constellation points in two different modes is $2a$. Hence, we can define the amplitude ratio for the interleaved (2,2)-PAM constellation as $p_2 = 2a/(2a+b)$. By finding optimal values for p_1 and p_2, the error performance of DM-PIM transmission can be optimized.

III. Experimental Results

To evaluate and compare the performance of DM-PIM with other benchmark scheme in OWC systems, hard experiments are conducted in a proof-of-concept PDM-OWC system in lab environments. Fig. 3 depicts the experimental setup of the PDM-OWC system using two red LDs. As we can see, the transmitted signals are first generated offline by MATLAB, which are then sent to a two-channel arbitrary waveform generator (AWG, TektronixAFG31102). After that, a DC bias current of 85 mA is combined with each of the two AWG output signals via a bias tee. Subsequently, the two combined signals are used to drive two red LDs (Ushio HL63603TG), and the generated optical signals further pass through two orthogonal polarizers. At the receiver side, a polarizer and an avalanche photodiode

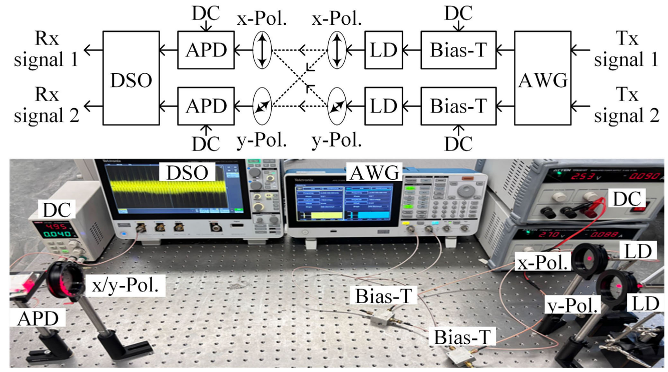

Fig. 3. Experimental setup of the PDM-OWC system using two red LDs.

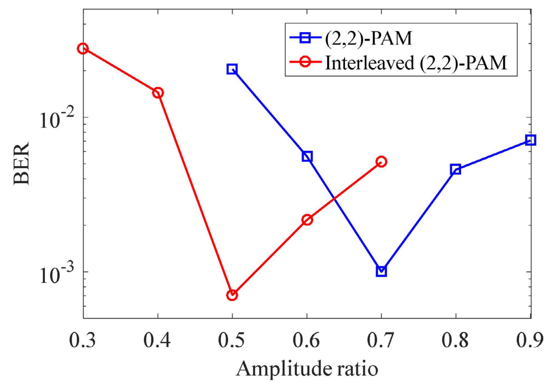

Fig. 4. BER vs. amplitude ratio for DM-PIM with (2,2)-PAM and interleaved (2,2)-PAM.

(APD, Hamamatsu C12702-12) are utilized together to detect the optical signal at two receiver positions. The detected electrical signals are captured by a digital storage oscilloscope (DSO, TektronixMDO32), and the resultant digital signals are further processed offline in MATLAB. In the experimental setup, the spacing between two red LDs is 10 cm, the spacing between two receiver positions is 10 cm, and the transmission distance is 93 cm. The following schemes are considered for performance comparison including DM-PIM with (2,2)-PAM and interleaved (2,2)-PAM, SM-PIM with 4-PAM, and PDM with 2-PAM and 4-PAM in x-polarization and y-polarization channels respectively. The error performance of the OWC system using different transmission schemes is evaluated in terms of AWG peak-to-peak voltage (Vpp), overall data rate of the system and the polarization offset angle due to polarization misalignment.

We first evaluate the impact of amplitude ratio for (2,2)-PAM and interleaved (2,2)-PAM on the performance of DM-PIM in the PDM-OWC system. Fig. 4 shows the bit error rate (BER) vs. amplitude ratio for DM-PIM with (2,2)-PAM and interleaved (2,2)-PAM, where the AWG sampling rate is 100 MSa/s, the DSO sampling rate is 500 MSa/s and the Vpp is 100 mV. As we can see, there exist optimal amplitude ratios to minimize BER for both (2,2)-PAM and interleaved (2,2)-PAM. Specifically, the optimal amplitude ratios for (2,2)-PAM and interleaved (2,2)-PAM to achieve minimum BERs are 0.7 and 0.5, respectively. In the following, the obtained optimal amplitude ratios are applied for performance evaluation of DM-PIM in the PDM-OWC system.

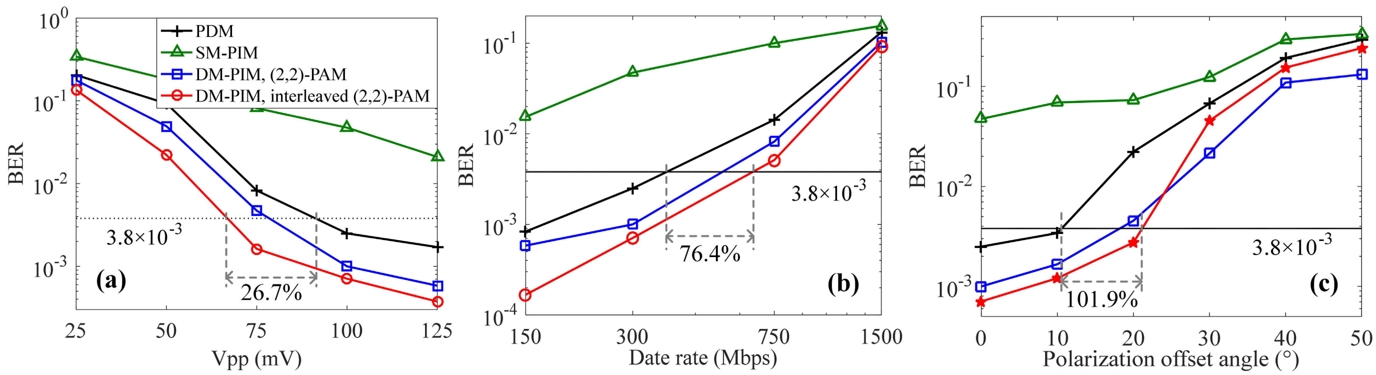

Fig. 5. Experimental results: (a) BER vs. Vpp, (b) BER vs. date rate, and (c) BER vs. polarization offset angle for different schemes.

In our future work, we will analytically derive the optimal amplitude ratios for DM-PIM by formulating a closed-form BER approximation with respect to the adopted dual-mode constellation design.

We further compare the BER performance of the OWC system employing different transmission schemes with ideal polarization alignment. Fig. 5(a) shows the BER versus Vpp where the AWG sampling rate is 100 MSa/s and the DSO sampling rate is 500 MSa/s. As can be seen, with the increase of Vpp, the BER of all four schemes gradually decreases. More specifically, SM-PIM cannot reach the 7% forward error correction (FEC) coding limit of BER = 3.8×10^{-3} within the Vpp range from 25 to 125 mV, due to its low spectral efficiency. For conventional PDM, a Vpp of 91.1 mV is required to reach BER = 3.8×10^{-3}. Moreover, DM-PIM with (2,2)-PAM outperforms PDM and DM-PIM with interleaved (2,2)-PAM achieves the best BER performance among all the four schemes. Compared with PDM, a Vpp reduction of 26.7% is achieved by DM-PIM with interleaved (2,2)-PAM to reach BER = 3.8×10^{-3}. Fig. 5(b) shows the BER versus data rate where the Vpp is set to 100 mV. It can also be found that DM-PIM with interleaved (2,2)-PAM obtains the highest data rate of 651.9 Mbps, which is corresponding to a substantial 76.4% rate improvement in comparison to PDM.

Moreover, we further study the impact of polarization misalignment on the BER performance of the OWC system using different transmission schemes. Fig. 5(c) characterizes the BER versus polarization offset angle, where the AWG sampling rate is 100 MSa/s, the DSO sampling rate is 500 MSa/s and the Vpp is 100 mV. It can be seen that the BER is gradually degraded with a larger polarization offset angle which indicates more severe inter-channel crosstalk between two orthogonal polarization channels. Particularly, a small polarization offset angle of 10.5° can only be supported by PDM, while the polarization offset angle is enlarged to 21.3° for DM-PIM with interleaved (2,2)-PAM, which is corresponding to a polarization offset angle extension of 101.9%. Hence, DM-PIM with interleaved (2,2)-PAM is much more robust against polarization misalignment than PDM.

IV. Conclusion

In this Letter, we have proposed and experimentally demonstrated a DM-PIM scheme for performance enhancement of PDM-OWC systems. The introduction of DM-IM in the polarization domain and the optimization of dual-mode PAM constellation can not only increase the overall spectral efficiency but also enhance the robustness against polarization misalignment in PDM-OWC systems. It is verified by the obtained experimental results that a rate improvement of 76.4% and a polarization offset angle extension of 101.9% can be achieved by DM-PIM with interleaved (2,2)-PAM in comparison to PDM. Therefore, the proposed DM-PIM scheme is very promising for bandlimited PDM-OWC systems.

References

[1] N. Chi, Y. Zhou, Y. Wei, and F. Hu, “Visible light communication in 6G: Advances, challenges, and prospects,” *IEEE Veh. Technol. Mag.*, vol. 15, no. 4, pp. 93–102, Dec. 2020.

[2] N. Chi, Y. Zhou, S. Liang, F. Wang, J. Li, and Y. Wang, “Enabling technologies for high-speed visible light communication employing CAP modulation,” *J. Lightw. Technol.*, vol. 36, no. 2, pp. 510–518, Jan. 15, 2018.

[3] C. Chen et al., “Digital pre-equalization for OFDM-based VLC systems: Centralized or distributed?” *IEEE Photon. Technol. Lett.*, vol. 33, no. 19, pp. 1081–1084, Oct. 15, 2021.

[4] C. Chen et al., “OFDM-based generalized optical MIMO,” *J. Lightw. Technol.*, vol. 39, no. 19, pp. 6063–6075, Oct. 1, 2021.

[5] W. Liu, Z. Ye, N. Huang, S. Li, and Z. Xu, “Multilevel polarization shift keying modulation for turbulence-robust underwater optical wireless communication,” *Opt. Exp.*, vol. 31, no. 5, pp. 8400–8413, 2023.

[6] X. Li, J. Yu, J. Zhang, Z. Dong, and N. Chi, “Doubling transmission capacity in optical wireless system by antenna horizontal-and vertical-polarization multiplexing,” *Opt. Lett.*, vol. 38, no. 12, pp. 2125–2127, 2013.

[7] E. Basar and E. Panayirci, “Optical OFDM with index modulation for visible light communications,” in *Proc. 4th Int. Workshop Opt. Wireless Commun. (IWOW)*, Sep. 2015, pp. 11–15.

[8] A. A. Purwita, A. Yesilkaya, M. Safari, and H. Haas, “Generalized time slot index modulation for optical wireless communications,” *IEEE Trans. Commun.*, vol. 68, no. 6, pp. 3706–3719, Jun. 2020.

[9] X. Zhong, C. Chen, Y. Zhao, M. Liu, C. He, and H. Haas, “Dual-mode spatial index modulation for MIMO-OWC,” *Opt. Lett.*, vol. 49, no. 2, pp. 334–337, 2024.

[10] X. Cai, W. Xu, S. Hong, and L. Wang, “Dual-mode differential chaos shift keying with index modulation,” *IEEE Trans. Commun.*, vol. 67, no. 9, pp. 6099–6111, Sep. 2019.

[11] X. Cai, W. Xu, L. Wang, and G. Chen, “Towards high-data-rate noncoherent chaotic communication: A multiple-mode differential chaos shift keying system,” *IEEE Trans. Wireless Commun.*, vol. 20, no. 8, pp. 4888–4901, Aug. 2021.

[12] Y. Nie, C. Chen, Z. Zeng, X. You, and G. Shen, “Multi-mode index modulation aided multi-band CAP with balanced pairwise coding for bandlimited VLC systems,” *J. Lightw. Technol.*, vol. 43, no. 5, pp. 2053–2066, Mar. 1, 2025.

[13] T. Mao, R. Jiang, and R. Bai, “Optical dual-mode index modulation aided OFDM for visible light communications,” *Opt. Commun.*, vol. 391, pp. 37–41, Apr. 2017.